Fatigue-cracking characteristics of a copper bicrystal when slip bands transfer through the grain boundary

Z.F. Zhang [a,b,*], Z.G. Wang [a]

[a] Shenyang National Laboratory for Materials Science, Institute of Metal Research, Chinese Academy of Sciences, Shenyang 110016, People's Republic of China

[b] IFW Dresden, Institute for Metallic Materials, PO Box 270016, D-01171 Dresden, Germany

Abstract

We reported the fatigue cracking characteristics of a special copper bicrystal with a tilt Σ 19b grain boundary (GB) and a coplanar primary slip system between the two grains. It is found that the primary slip bands of the two adjacent grains have a good continuation across the GB on the four surfaces of the bicrystal specimen in the axial plastic strain range of 1.5×10^{-4}–2.13×10^{-3}. It indicates that the surface slip bands had transferred through the GB during cyclic deformation. When cyclic plastic strain was continued to be applied on the bicrystal specimens, fatigue cracks always initiated and propagated along the GB at all the applied strain amplitudes. By using electron channeling contrast (ECC) technique in scanning electron microscopy (SEM), the dislocation patterns near the GB of the bicrystal were observed. The ladder-like persistent slip bands (PSBs) did not transfer through the GB continuously, no matter what the surface or the common primary slip plane of the bicrystal. Instead, a dislocation affected zone (DAZ) or piling-up of dislocations near the GB was observed. Based on the results above, the fatigue cracking mechanism of the bicrystal was discussed and the GB cracking was attributed to the difference in the slip directions of the two adjacent grains.
© 2002 Elsevier Science B.V. All rights reserved.

1. Introduction

Grain boundaries (GBs) play a critical role in determining the mechanical properties of materials, since they can block the motion of dislocations and thus affect the plastic behavior of the deformed materials. GBs can also serve as the origin of fatigue cracking and further become the fracture paths in polycrystalline materials [1–3]. Recently, the fatigue cracking phenomenon along large-angle GBs were observed in different copper bicrystals with parallel, perpendicular and inclined GBs [4–9]. The intergranular fatigue cracking of the bicrystals was attributed to the PSB-GB damage mechanism [2,10,11], since the slip planes between two adjacent grains often intersected at large angles at the GBs, which resulted in the piling-up of dislocations [12,13]. In another group of test, we fabricated copper columnar crystals, which contained some low-angle GBs. After cyclic deformation, it is interesting to find that the low-angle GBs did not initiate fatigue cracks until fatigue failure [14]. Instead, fatigue cracks always nucleated and propagated along the activated PSBs no matter whether the low-angle GBs are perpendicular or parallel to the stress axis. PSBs can transfer through the low-angle GBs and no piling-up of dislocations was observed during cyclic deformation of the columnar crystals [15] since the misorientation between the adjacent grains is quite small. Therefore, the discontinuity of the PSBs across GBs was considered as an important factor for the intergranular cracking. In the present work we prepared a copper bicrystal, in which the GB is a large-angle boundary, but the primary slip

* Corresponding author. Tel.: +49-351-465-9766; fax: +49-351-465-9541

E-mail address: z.f.zhang@ifw.dresden.de (Z.F. Zhang).

planes of the two adjacent grains are coplanar so as to continuity the succession of the slip bands across the GB.

2. Experimental procedure

A bicrystal was grown from OFHC copper of 99.999% purity by the Bridgman method. As shown in Fig. 1(a), the two primary (111) slip planes of the two grains in the copper bicrystal are coplanar. By electron backscatter diffraction (EBSD) technique, the rotation angle was determined between the two grains as 46.2° about the common [111] rotation axes. Therefore, the slip directions b_1 and b_2 of the primary slip system of the two grains enclose an angle of 13.8°, as illustrated in Fig. 1(b). A group of bicrystal specimens with a GB plane tilted to the tensile axis were prepared. The gauge dimension of the bicrystal specimen is $16 \times 6 \times 6$ mm

and the crystallographic orientations of the two grains in the bicrystal are

$$G_1 = \begin{bmatrix} -13 & 4 & -5 \\ 11 & -15 & -4 \\ -11 & -20 & 2 \end{bmatrix} \text{ and } G_2 = \begin{bmatrix} -12 & 18 & 3 \\ 5 & -2 & 20 \\ 30 & 7 & -2 \end{bmatrix}$$

Here, the axis orientations of the two grains are $G_1[\bar{4}\ 15\ 20]$ and $G_2[18\ \bar{2}\ 7]$, which are typical single slip orientations. Therefore, the Schmid factors of the primary slip systems of the two grains are 0.47 (Ω_{G_1}) and 0.49 (Ω_{G_2}), respectively. After careful polishing of the bicrystal specimens, cyclic push–pull tests were performed on a Shimadzu servo-hydraulic testing machine under constant plastic strain control at room temperature in air. A triangle waveform with a frequency range of 0.1–1 Hz was used. The applied axial plastic strain amplitudes ($\Delta\varepsilon_{pl}/2$) were in the range of 1.5×10^{-4}–2.13×10^{-3}. During cyclic deformation, the slip morphology on the specimen surfaces was examined
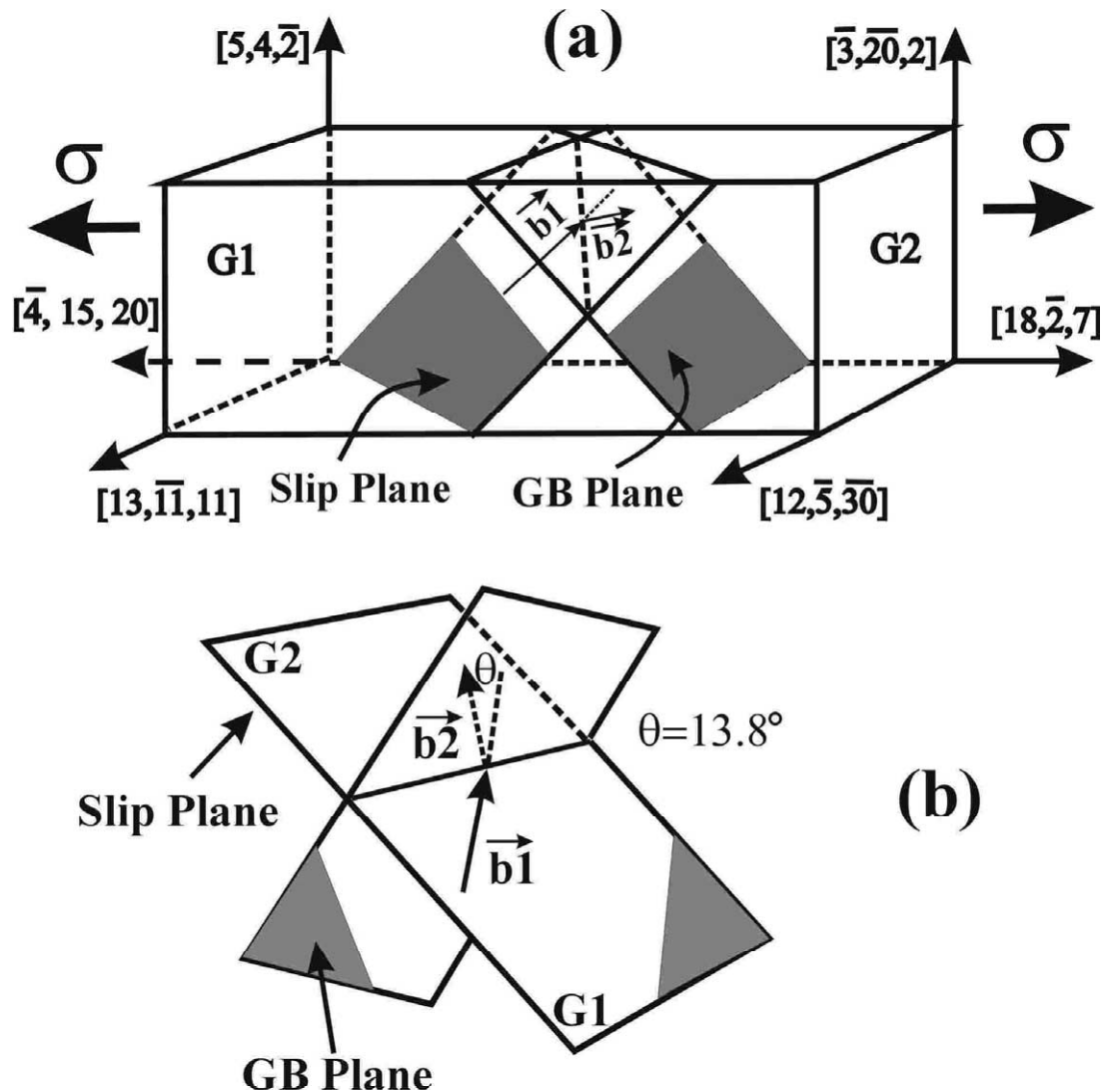
Fig. 1. Crystallographic relationship between primary slip plane, GB and stress axis in the bicrystal.

by scanning electron microscopy (SEM). The fatigue tests were terminated at the initiation of fatigue crack on the specimen surfaces. Meanwhile, the dislocation patterns near the GB were observed by electron channeling contrast (ECC) technique in a Cambridge S360 SEM. Similar to the image technique reported by Schwab et al. [16], an inverted imaging mode is adopted in the present investigation so that the ECC micrographs are in accord with the TEM micrograph under bright field imaging conditions.

3. Results and discussion

In the applied axial plastic strain range all bicrystal specimens exhibited an initial cyclic hardening and cyclic saturation behavior. The axial saturation stresses of all bicrystal range from 61.6 to 63.5 MPa, the detailed results can be seen in Table 1. Hence the cyclic stress–strain response of the present bicrystal is quite similar to the copper single crystals oriented for single-slip [17]. Since the Schmid factors of the two grains are known, the resolved saturation shear stresses τ_{G_1} and τ_{G_2} applied on the primary slip planes of grains G_1 and G_2 can be calculated by the following equations:

$$\tau_{G_1} = \sigma_B \Omega_{G_1} \tag{1}$$

$$\tau_{G_2} = \sigma_B \Omega_{G_2} \tag{2}$$

Here, σ_B is the axial saturation stress of the bicrystal; Ω_{G_1} and Ω_{G_2} are the Schmid factors of the primary slip systems of grain G_1 and G_2 and are equal to 0.47 and 0.49, respectively. The calculated results of τ_{G_1} and τ_{G_2} are shown in Fig. 2 and they are also listed in Table 1. The resolved saturation shear stresses of grain G_1 and G_2 are in the ranges of 28.9–29.8 MPa and 30.2–31.1 MPa, respectively, which are approximately equal to the resolved saturation shear stress (28–30 MPa) of the single-slip copper single crystal [17] and of columnar copper crystals containing low-angle GBs [15]. This indicates that the large-angle GB has little effect on the cyclic stress-strain response of the bicrystal, which is similar to the effect of low-angle GBs.

By observing the surface slip morphologies of the copper bicrystals deformed at different strain amplitudes, the damage mechanism was identified. It was found that in both grains the common primary slip bands were activated on the whole surface, including the
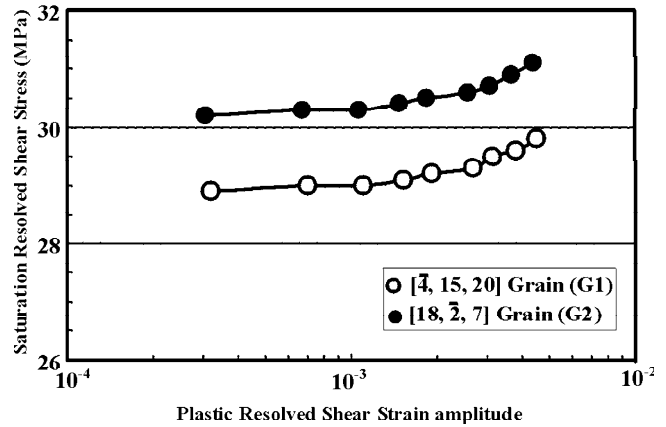
Fig. 2. Cyclic stress–strain curves of the grains G_1 and G_2 in the bicrystal.

vicinity of the GB. Fig. 3(a) and (b) show the slip morphologies near the GB on two surfaces of the bicrystal specimen. It is worth noting that these slip bands have a continuous relationship across the GB, whereas secondary slip bands was not observed. This indicates that the primary slip bands had transferred through the GB during cyclic deformation, which can be attributed to the special crystallographic relationship of the bicrystal, as illustrated in Fig. 1. The slip deformation feature of the present bicrystal is similar to that in the fatigued columnar copper crystals containing low-angle GBs. However, it was not observed before that slip bands can transfer through a random large-angle GB in other fatigued bicrystals [4–9,12–14]. With increasing strain amplitude or cycle number, it seems that some plastic strain incompatibility occurred near the GB, as shown in Fig. 3(c). Therefore, it can be concluded that the slip bands on the surface can transfer through the GB of the bicrystals with a coplanar primary slip system, whereas some plastic strain incompatibility may still occur near the GB at higher strain amplitudes or higher cycles.

When cyclic deformation was continued, it was observed that fatigue crack always initiated at the GB, as shown in Fig. 4(a). Beside the intergranular crack, the PSBs within the two grains still have a one-to-one relationship and the secondary slip bands were not activated yet. So the effect of secondary slip bands on the GB cracking can be excluded. With further cyclic deformation, the intergranular crack gradually propagated along the GB, finally leading to the intergranular

Table 1
Saturation stresses of the [$\bar{4}$ 15 20]/[18 $\bar{2}$ 7] bicrystal and the resolved shear stress of the adjacent grains at different strain amplitudes

$\varepsilon_{pl} \times 10^{-4}$	1.5	3.3	5.2	7.2	9.0	12.6	15.0	18.0	21.3
$\sigma_{[\bar{4}\ 15\ 20]/[18\ \bar{2}\ 7]}$ (MPa)	61.6	61.8	61.7	61.9	62.1	62.4	62.7	63.0	63.5
$\tau_{[\bar{4}\ 15\ 20]}$ (MPa)	28.9	29.0	29.0	29.1	29.2	29.3	29.5	29.6	29.8
$\tau_{[18\ \bar{2}\ 7]}$ (MPa)	30.2	30.3	30.3	30.4	30.5	30.6	30.7	30.9	31.1
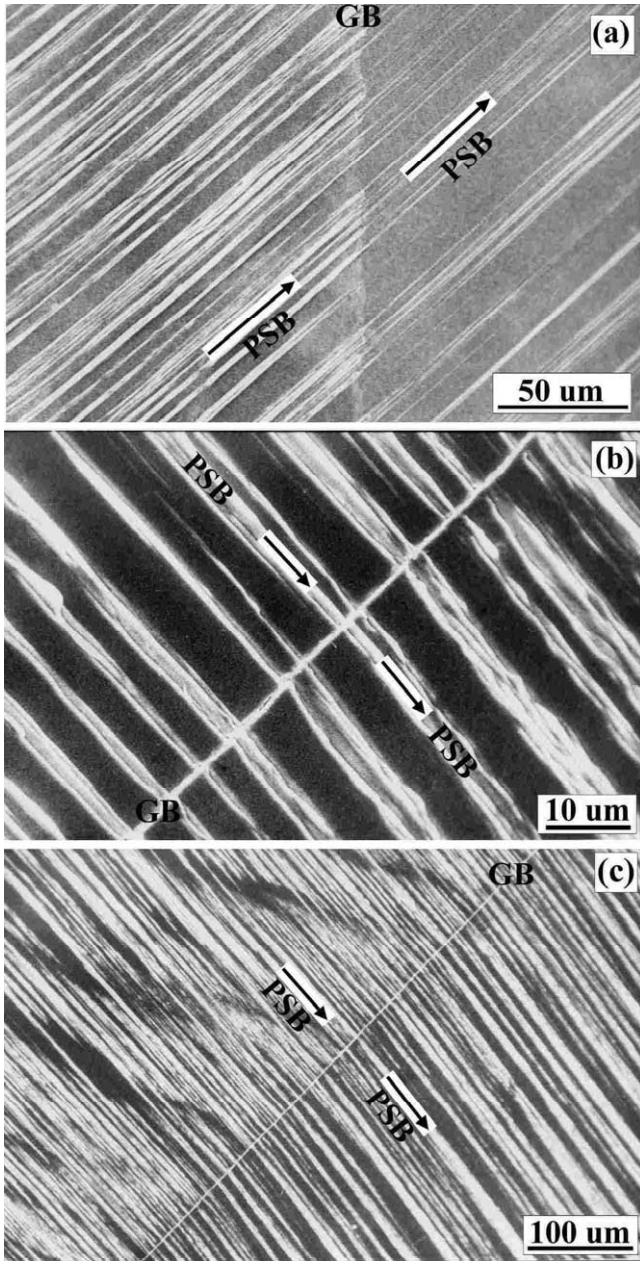
Fig. 3. Slip morphologies near the GB on the two surfaces of the bicrystal specimen.

Fig. 4. Fatigue cracking along the GB on the surfaces of the bicrystal specimen.

fracture along the whole GB, as shown in Fig. 4(b). The present results show that, although the interaction of PSBs with the GB in the present bicrystal is similar to that in columnar crystals containing low-angle GBs [15], eventually fatigue cracking along the present GB is still inevitable. It indicates that the intergranular cracking characteristics of the present bicrystal is identical with those of the copper bicrystals with large-angle GBs parallel or perpendicular to the stress axis [4–9], but is contrary to the fatigue cracking of the columnar crystals containing low-angle GBs, in which PSBs are the preferential sites for the nucleation of fatigue cracks [14].

For better understanding the fatigue cracking mechanism of the bicrystal, the dislocations and the interactions of PSBs with the GB were carefully observed by the SEM-ECC technique. It was found that the ladder-like PSBs and the vein-like dislocations had formed in the two grains, indicating that the deformation mechanism of the two component grains is identical with the copper single crystals [18,19]. Fig. 5(a) shows the interaction of PSBs with the GB on the specimen surface. It can be seen that the ladder-like dislocations are discontinuous across the GB. In the lower grain, the ladder-like PSBs terminated at the GB, however, the dislocations did not show a ladder-like feature in the upper grain. The difference in the dislocation patterns should be attributed to the difference in the orientation of the two grains, as illustrated in Fig. 1. By careful observation, it can be seen that there exists the piling-up of dislocations at the GB, as indicated by the arrows. This implies that the dislocation patterns within the PSBs of the two grains are discontinuous. After that, the bicrystal specimen was cut along the common primary slip plane and was further observed by the SEM-ECC technique. The results are shown in Fig. 5(b) and (c), obviously, the dislocation pattern beside the GB is also discontinuous and a dislocation-affected zone (DAZ) with 10 μm in width
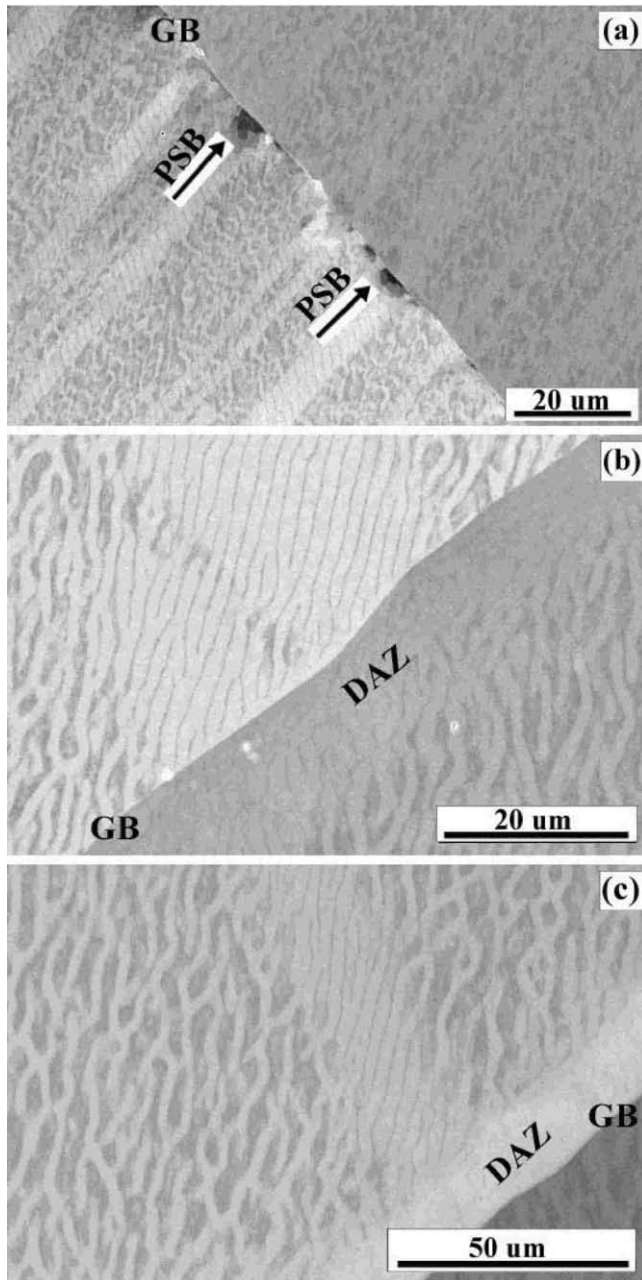
Fig. 5. Dislocation patterns observed by the SEM-ECC technique (a) on the surface of the specimen; (b) and (c) on the common primary slip plane.

the two grains are obviously different, as shown in Fig. 1.

Based on the observations above, the difference in the fatigue cracking mechanism between large-angle and small-angle GBs can be explained by the differences in crystallographic features. First, from Fig. 2, it is clear that there is a stress difference in the resolved saturation shear stresses τ_{G_1} and τ_{G_2} of the grains due to the
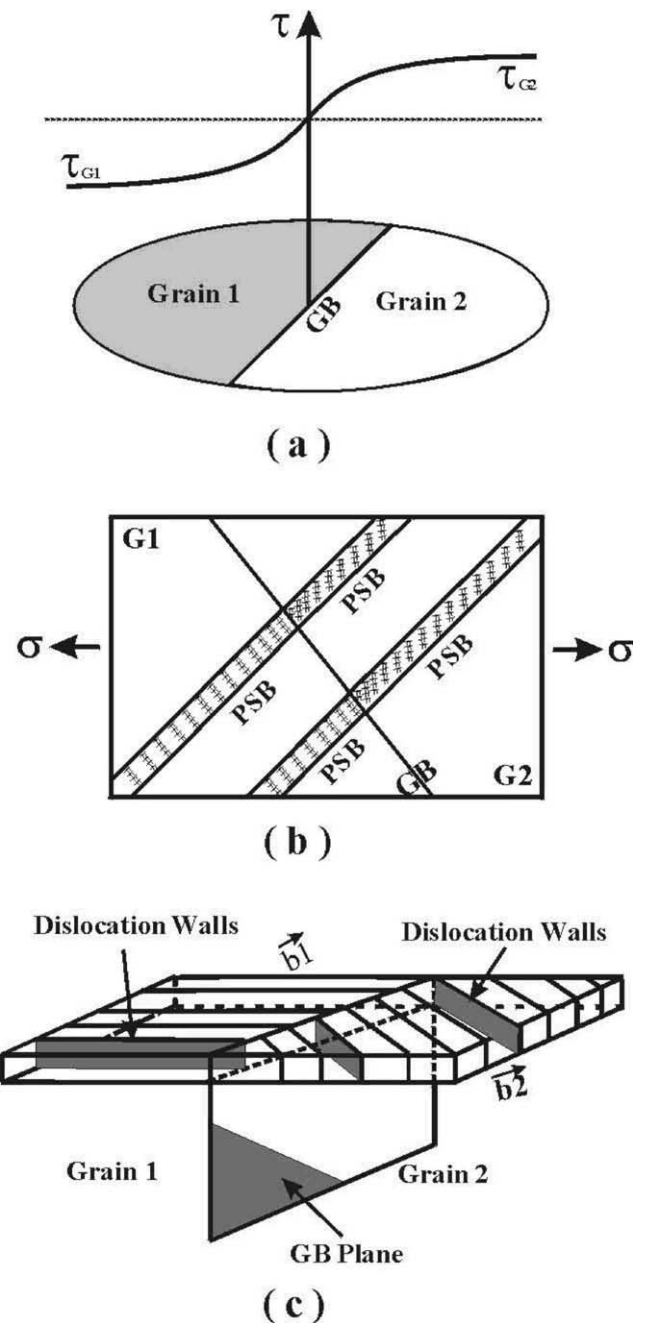
Fig. 6. Schematic illustration of the interaction of PSBs and dislocations with the GB in the bicrystal. (a) Stress distribution within grain G_1 and G_2 on the common primary slip plane. (b) Interaction of surface slip bands with the GB. (c) Interaction of dislocations with the GB on the common primary slip plane.

appeared near the GB. It is very similar to the dislocation-free zone (DFZ) observed by TEM technique in a $[\bar{3}45]/[\bar{1}17]$ bicrystal [6] and polycrystals [20]. The observations above are not consistent with the surface slip bands in Fig. 3, indicating that the ladder-like dislocations within PSBs cannot completely transfer through the GB despite of the two grains of the bicrystal having a coplanar primary slip system. It is nevertheless acceptable since the primary slip directions $\mathbf{b_1}$ and $\mathbf{b_2}$ of

difference in the Schmid factors. Therefore, the stress distribution of the saturation resolved shear stresses τ_{G_1} and τ_{G_2} on the common primary slip planes of the grains can be illustrated as in Fig. 6(a). Near the GB, obviously, there will be a stress gradient and the stress difference near the GB will be:

$$\Delta\tau = \tau_{G_2} - \tau_{G_1} = \sigma_B(\Omega_{G_2} - \Omega_{G_1}) \tag{3}$$

During cyclic deformation of the bicrystal, the stress difference will become the resistance of the GB to the slip deformation of the two grains. From the observed surface slip bands in Fig. 3, the interaction of PSBs with the GB on the surface is illustrated schematically in Fig. 6(b). The figure can explain the discontinuity of ladder-like dislocations on the surfaces due to the difference in the orientations of the two grains. If we consider the deformation processes of the PSBs on their common slip plane, as shown in Fig. 6(c), the ladder-like dislocation walls will slip along the directions $\mathbf{b_1}$ and $\mathbf{b_2}$, which are perpendicular to the dislocation walls. During cyclic deformation of the bicrystal, the PSBs within the two grains will impinge at the GB. Since the Burgers vectors $\mathbf{b_1}$ and $\mathbf{b_2}$ of the two PSBs within the grains are not identical (there is an angle of misoreintation 13.8°), the dislocations carried by each PSB cannot transfer through the GB continuously and were piled up at the GB, as seen in Fig. 5. During cyclic deformation of the bicrystal, the GB was impinged by the PSBs to form the piling-up of dislocations and there is a stress gradient near the GB. Piling up dislocations at the GB, inter-granular cracking is inevitable in the bicrystal. However, for the columnar crystals containing low-angle GBs, the dislocations can be easily moved into the adjacent grains by the coplanar PSBs [15] due to the small misorientation between the neighboring grains. As a result, no piling-up of dislocations was observed near the low-angle GBs. Therefore, the dislocation will be moved into the crystal surface, leading to the surface roughness and the nucleation of fatigue cracks along the PSB. In essence, the intergranular fatigue cracking of the present bicrystal is identical with all the other bicrystals with a random large-angle GB, i.e. the piling-up mechanism of dislocations.

4. Conclusions

The cyclic saturation stress of the copper bicrystal with a coplanar primary slip system ranges from 61.6 to 63.5 MPa in the axial plastic strain range of 1.5×10^{-4}–2.13×10^{-3}. If taking the Schmid factors of two grains into account, the cyclic stress–strain curve (CSSC) of the bicrystal is close to a copper single crystal with single-slip. The surface slip bands can transfer through the GB on the four surfaces of the bicrystal specimen, indicating that the GB did not affect the slip deformation feature of the bicrystal. However, the ladder-like PSBs are discontinuous beside the GB both on the specimen surface and on the common slip plane. A dislocation-affected zone (DAZ) or piling-up of dislocations was observed near the GB, indicating that the PSBs cannot completely transfer through the GB which can be explained by the difference in the slip directions of the two grains. The GB is the preferential site for the nucleation of fatigue cracks in the special bicrystal specimen. The intergranular fatigue cracking mechanism can be attributed to the piling-up of dislocations at the GB and the resistance of the GB to the PSBs, which were resulted from the difference in the slip directions of the two grains.

References

[1] F.L. Liang, C. Laird, Mater. Sci. Eng. A117 (1989) 83.
[2] W. Liu, M. Bayerlein, H. Mughrabi, A. Day, P.N. Quested, Acta Metall. Mater. 40 (1992) 1763.
[3] H.L. Huang, N.J. Ho, Mater. Sci. Eng. A298 (2001) 251.
[4] P. Peralt, C. Laird, Acta Mater. 45 (1997) 3029.
[5] P. Peralt, C. Laird, Acta Mater. 46 (1998) 2001.
[6] Y.M. Hu, Z.G. Wang, Acta Mater. 45 (1997) 2655.
[7] Y.M. Hu, Z.G. Wang, Int. J. Fatigue 20 (1998) 634.
[8] Z.F. Zhang, Z.G. Wang, Y.M. Hu, Mater. Sci. Eng. A269 (1999) 136.
[9] Z.F. Zhang, Z.G. Wang, Y.M. Hu, Mater. Sci. Eng. A272 (1999) 412.
[10] H. Mughrabi, F. Ackermann, K. Herz, ASTM STP 81 (1981) 5.
[11] H-J. Christ, Mater. Sci. Eng. A117 (1989) L25.
[12] Z.F. Zhang, Z.G. Wang, Acta Mater. 46 (1998) 5063.
[13] Z.F. Zhang, Z.G. Wang, Phil. Mag. Lett. 78 (1998) 105.
[14] Z.F. Zhang, Z.G. Wang, S.X. Li, Fatigue Fract. Eng. Mater. Struct. 21 (1998) 1307.
[15] Z.F. Zhang, X.W. Li, H.H. Su, Z.G. Wang, J. Mater. Sci. Technol. 14 (1998) 211.
[16] A. Schwab, J. Bretschneider, C. Buque, C. Blochwitz, C. Holste, Phil. Mag. Lett. 74 (1996) 449.
[17] H. Mughrabi, Mater. Sci. Eng. 33 (1978) 207.
[18] A.T. Winter, Phil. Mag. 30 (1974) 719.
[19] J.M. Finney, C. Laird, Phil. Mag. 31 (1975) 339.
[20] T. Luoh, C.P. Chang, Acta Mater. 44 (1996) 2683.